

Supporting information for

Nanocrystal Superlattices with Thermally Degradable Hybrid Inorganic-Organic Capping Ligands

Maksym V. Kovalenko^{}, Maryna I. Bodnarchuk, Dmitri V. Talapin^{*}*

Department of Chemistry and James Frank Institute, University of Chicago, Chicago, IL 60637

e-mail: mvkovalenko@uchicago.edu, dvtalapin@uchicago.edu

Materials and methods.

I. Chemicals.

Na₂S·9H₂O (≥98%, Aldrich), Pd acetylacetonate (Pd(acac)₂, 99%, Aldrich), Trioctylphosphine oxide (TOPO, 99%, Aldrich), trioctylphosphine (TOP, 97%, Strem), oleylamine (OLA, 70%, Aldrich), didodecyldimethylammonium bromide (DDAB, 98%, Fluka), dodecanethiol (DT, 98%, Aldrich), tetraline (1,2,3,4-tetrahydronaphthalene, 97%, Aldrich), tert-butylamine-borane complex (TBAB, Aldrich, 97%), Iron pentacarbonyl (Fe(CO)₅, 99.999%, Aldrich), 1,2-tetradecanediol (90%, Aldrich), dioctyl ether (>97%, Aldrich), hexadecylamine (HDA, 90%, Fluka), tetradecylphosphonic acid (TDPA, 99%, Polycarbon), octadecylphosphonic acid (ODPA, 99%, Polycarbon), propylphosphonic acid (PPA, 95%, Aldrich), dimethylcadmium (97%, Strem), Selenium (powder, 99.99%, Aldrich), Lead acetate trihydrate (PbAc₃·3H₂O, Aldrich), Cadmium oxide (99.995%, Aldrich), oleic acid (OA, 90%, Aldrich), squalane (99%, Aldrich), 1-octadecene (ODE, 90%, Aldrich), Gold(III) chloride (99.99%, Aldrich), Gold(III) chloride trihydrate (HAuCl₄·3H₂O, ≥99.9%, Aldrich), Platinum acetylacetonate (98%, Strem), sodium sulfide nonahydrate (Na₂S·9H₂O, 99.99%, Aldrich), ammonium sulfide (40-48% solution in water, Aldrich), ammonium hydroxide (28-30% of NH₃, Aldrich), arsenic(III) sulfide (As₂S₃, 99.9%, Alfa Aesar), formamide (FA, 99%, Aldrich), and various solvents were used as received. Octadecene was dried at 140°C for 2 hours under vacuum and stored in a nitrogen glovebox.

II. Synthesis of colloidal nanocrystals.

4.2 nm Pd NCs were synthesized based on the protocols reported by Hyeon *et al.*¹ with some modifications. The flask containing 10 mL OLA and 0.25 g TOPO was heated to 50 °C under vacuum for 30 min. 2 mL of the OLA-TOPO mixture were withdrawn and mixed with a solution of 0.1 g Pd(acac)₂ in 0.3 mL TOP (prepared in a glovebox) and the resulting mixture was injected into the reaction flask. The flask was heated to 100 °C under vacuum. The solution was heated under nitrogen to 250 °C at the rate of ~3 °C/min, kept at 250 °C for 30 min and cooled to room temperature. To wash Pd NCs, 2 mL toluene and 30 mL ethanol were added followed by centrifugation. Collected precipitate of NCs was redispersed in 3 mL toluene.

3.8 nm FePt NCs were synthesized by slightly modified method of Sun *et al.*² Platinum acetylacetonate (197 mg, 0.5 mmol), 1,2-tetradecanediol (345 mg, 1.5 mmol) and dioctyl ether (20 mL) were mixed and heated to 100°C under airless conditions. At this temperature, a solution of oleic acid (0.16 mL, 0.5 mmol), oleylamine (0.17mL, 0.5mmol) and Fe(CO)₅ (0.13 mL, 1 mmol) was injected, and the mixture

was further heated to reflux (295°C). The refluxing was continued for 30 min. Then the reaction mixture was cooled to room temperature. The black product was precipitated by adding toluene (10 ml) and ethanol (60 ml) and separated by centrifugation. The black precipitate was redissolved in toluene (~10 ml) in the presence of oleic acid (10 µL) and oleylamine (10 µL), and then centrifuged to remove any insoluble NCs or byproducts. The NCs were additionally precipitated by adding 30-40 ml ethanol followed by centrifugation. The NCs were redispersed in toluene.

4 nm OLA-capped Au NCs were prepared according to the method of S. Sun et al.,³ with minor modifications. A mixture of 10 ml tetraline, 10 mL oleylamine and 0.1 g HAuCl₄·3H₂O were mixed at room temperature and stirred for 20 min under nitrogen purge. A solution containing 0.5 mmol TBAB complex (0.0435 g), 1 ml oleylamine and 1 ml tetraline was injected into the precursor solution. Solution turned yellow to dark purple in 2-5 s. Stirring was continued for 30 minutes before the washing procedure. 40 ml acetone and 8 mL methanol were added to precipitate the NCs, followed by centrifugation. The precipitate of Au NCs was redispersed in 8 mL toluene. A minimal amount of methanol was added to precipitate Au NCs. After centrifuging, Au NCs were redispersed in toluene.

8.1-nm and 10 nm CdSe NCs capped with TDPA were synthesized using Cd(CH₃)₂ and TOPSe as precursors according to previously reported procedures with slight modifications.^{4,5} Note that the growth kinetics was found to be somewhat sensitive to the batch number of the TOPO (99%, Aldrich) and has to be adjusted by taking aliquots. For large NC sizes, the size-distribution appears different from batch to batch, and can be easily refined by size-selective precipitation.

CdS nanorods. We used a slightly modified version of the method developed by Alivisatos group.⁶ In a typical synthesis of 4×28 nm nanorods, a mixture of TOPO (3.5 g), CdO (209 mg, 1.6 mmol), OHPA (1.07 g, 3.20 mmol) and PPA (15 mg, 0.12 mmol) was degassed under vacuum at 120 °C for 20 min and then heated to 320 °C under nitrogen to dissolve CdO. Afterwards, the reaction mixture was cooled to 120 °C and kept for 2 hours at that temperature under vacuum to dry the solution. The temperature was restored to 320 °C under nitrogen atmosphere. 2 g of TOP was added at 300 °C. 0.625 g of pure TOPS (prepared by reacting equimolar amounts of S and TOP at room temperature) was injected into the reaction flask at 320°C. The nanorod growth was terminated after 10 minutes by cooling the reaction flask. All nanorods showed excellent uniformity in width and length and well-structured optical absorption spectra. To isolate and purify as-synthesized CdS nanorods, a crude solution was mixed with toluene (15 mL), 10% solution of octylamine in hexane (10 mL) and acetone (10 mL). The resulting suspension was centrifuged at 12000g for 10 min. The precipitate was redispersed in a mixture of toluene (10-15 mL) with 10% solution of octylamine in hexane (15 mL) and precipitated again by adding ethanol. The dissolution/precipitation procedure was repeated one more time with addition of

octylamine, and then 2 times without addition of octylamine. Finally, CdS nanorods were dissolved in toluene forming a stable colloidal solution.

3-12 nm PbS NCs capped with oleic acid were synthesized according to the procedure developed by Hines *et al.*⁷

III. Replacement of the original organic ligands with hybrid inorganic-organic capping ligands.

$(\text{NH}_4)_3\text{AsS}_3$ ⁸ was prepared by dissolving 0.492 g As_2S_3 in a solution containing $(\text{NH}_4)_2\text{S}$ (0.86 mL, 40-48% in water) and 10 mL H_2O at room temperature. Na_3AsS_3 was prepared in the same way as $(\text{NH}_4)_3\text{AsS}_3$ by using Na_2S instead of $(\text{NH}_4)_2\text{S}$. Dry Na_3AsS_3 can be isolated as a powder by adding acetone, centrifuging and drying. The formation of AsS_3^{3-} was confirmed by electrospray ionization mass spectrometry (Figure S1).

The ligand exchange with AsS_3^{3-} ions was conducted as a heterogeneous reaction in the mixture of two largely or completely immiscible solvents of nonpolar and polar character, e.g. toluene-FA, leading to the complete phase transfer of NCs from the non-polar to the polar phase and the formation of colloiddally stable solutions. The MCC to NC molar ratio was in the range of 0.5-2, with lower MCC amounts used for larger NCs. All experiments were carried out in air. As an example of the preparation of AsS_3^{3-} -capped PbS NCs, a toluene solution of 3.7 nm oleic-acid capped PbS NCs (0.5 mL, 60 mg/mL, ~0.25 M referred to PbS formula unit) was mixed with FA (5 mL), toluene (5 mL) and Na_3AsS_3 in FA (0.5 mL, 50 mg/mL, ~0.21 M). Solution was stirred for 0.5-2 hours until the organic phase turned colorless and FA phase became dark brown. The upper organic phase was carefully removed. The FA phase was further purified by triple washing with toluene and filtered through a 0.45 μm PTFE filter. Residual toluene can be removed by drying in vacuum, if necessary. The resulting solution can be used for further functionalization with dodecyldimethyl ammonium (DDA^+). Furthermore, the solution of AsS_3^{3-} -capped PbS NCs can be purified from excess MCC by adding equal volume of acetonitrile, centrifuging and redispersing in pure FA.

To exchange Na^+ (NH_4^+) surface counterions with DDA^+ , the solution of AsS_3^{3-} -capped PbS NCs obtained as described above was mixed with DDAB in toluene (0.4 mL, 0.1 M) and 5 mL toluene, stirred until the completion of the phase transfer of PbS NCs from FA into toluene phase and formation of a stable colloidal solution. The following washing with water was applied to remove excess DDAB. Upon phase separation, the toluene phase was mixed with large amount of water (50 mL), vigorously shaken and centrifuged. The aqueous phase was discarded and the washing was repeated 1-2 times until both aqueous and toluene phases appeared completely clear. The resulting solutions were used for self-

assembly experiments. AsS_3^{3-} -DDAB-capped PbS NCs can be additionally purified by adding methanol until flocculation, centrifuging and redispersing NCs in toluene.

Tertiary alkylammonium salts were selected because of their pH-independent charging (unlike, secondary and ternary substituted salts), low-cost and low onset for thermal decomposition. As an additional benefit, there is an extensive prior art on their use in densely packed hydrophobic monolayers on aluminosilicates⁹⁻¹² or as templates for the formation of porous silica and zeolites.^{13,14} We tested different commercially available tertiary alkylammonium salts, containing methyl groups and various numbers of long alkyl chains ($\geq C_6$) per the head group (e.g. $1C_n$, $2C_n$, $4C_n$). In all cases, addition of the alkylammonium ions to FA or aqueous solution of MCC-capped NCs results in their strong association with MCC anions, leading to precipitation of NCs. The second stage, transfer from FA to toluene and formation of stable colloidal solution, is most critical and reflects the density and stability of the alkylammonium coating. Thus, the presence of 1-2 alkyl chains with $\geq C_{12}$ are needed to solubilize NCs in toluene or chloroform, which correlates with the onset for the formation of stable and dense monolayers on aluminosilicate surfaces (strong inter-chain van der Waals forces). Dialkyl ($2C_n$) substituted molecules generally performed better than $1C_n$, and $4C_n$, which can be best explained by the good match between the molecule cross section and the density of negatively charged surface sites.¹² Another important criterion is the solubility of tertiary alkylammonium bromides in chosen solvents. Those which contained chains with $\geq C_{16}$ are typically soluble in chloroform but not in toluene or hexane. We also compared long-term stability of resulting colloids. Overall, DDAB demonstrated the most convenient set of characteristics.

IV. Self-assembly of DDA^+ - AsS_3^{3-} -capped nanocrystals.

All self-assembly experiments were carried out using standard drying-mediated approach.^{15,16} Carbon-coated copper TEM grids (type-B, Ted Pella) were used as the substrates for self-assembly experiments. The grids were dipped in toluene for 15s to remove protective formvar coating, followed by drying on a filter paper. The grids were placed inside a tilted glass vial ($\sim 60^\circ$ tilt angle). $\sim 25 \mu\text{L}$ of a single component or binary NC solution with desired particle size and number ratio (the concentration $\sim 10^{14}$ NC cm^{-3}) were placed above the grid to cover it entirely. The solutions were prepared by diluting concentrated toluene solutions of NCs with tetrachloroethylene. Concentrations of NCs were estimated either photometrically for CdSe, PbS and PbSe using known extinction coefficients¹⁷⁻¹⁹ or gravimetrically for all other NCs. The vials were placed into nitrogen filled chamber at 50°C and left undisturbed for at least 12 hours to evaporate the solvent.

V. Materials characterization.

DLS and ζ -potential data were collected using a Zetasizer Nano-ZS (Malvern Instruments, UK). Colloidal solutions were filled into a quartz cuvette and the dip cell electrode assembly with Pd electrodes was used to apply an electric field to solution. A typical ζ -potential measurement included several scans of 100 runs each in the high-resolution mode. The concentration was optimized for each sample to achieve a >100 kcps count rate and the best signal-to-noise ratio.

Transmission electron microscopy (TEM) of the samples was performed using FEI Tecnai F30 microscope operated at 300 kV. Two-dimensional arrays of all studied NCs with original organic ligands and with $\text{DDA}^+\text{-AsS}_3^{3-}$ -coating were carefully analyzed to determine the mean NC size, interparticle distance and the ligand shell thickness. The initial NC core size for PbS and CdSe NCs was also determined from the energy of the first absorption peak.^{17,20} The average $\text{DDA}^+\text{-AsS}_3^{3-}$ -shell thickness was found to be 1.8 nm based on the difference between the mean interparticle distance in the hexagonally ordered arrays and the diameter of the NC core.

Thermogravimetric analysis (TGA) was conducted using Shimadzu TGA-50 thermal analyzer with a heating rate of 5 °C/min under nitrogen. Samples of dried NCs were kept under vacuum at 100 °C to remove chemi- and physisorbed molecules of water and solvents (e.g. formamide).

The absorption spectra of NC solutions were collected using a Cary 5000 UV-Vis-NIR spectrometer.

Fourier-transform infrared (FTIR) spectra were acquired in the transmission mode using a Nicolet Nexus-670 FTIR spectrometer with a resolution of 4 cm^{-1} , and averaging over 64 scans. For the measurements, thick films were deposited on KBr or CaF_2 crystal substrates (International Crystal Labs) by drying concentrated NC solutions. After the phase transfer and washing, Na_3AsS_3 -stabilized PbS NCs were precipitated by adding acetonitrile to their formamide solution and redispersed in neat formamide. Dried films were kept in a vacuum chamber at 110°C overnight to remove chemi- and physisorbed water and formamide molecules. The reference sample for FTIR measurements was prepared by drying oleic-acid capped PbS NCs from their toluene solution at room temperature and keeping sample at 110°C overnight. For quantitative comparison of different samples, same mass-per-substrate area was deposited (about 5 mg/cm^2) and the spectra were baseline-corrected.

Elemental analysis by the inductively coupled plasma optical emission spectroscopy (ICP-OES) was performed at the Analytical Chemistry Laboratory (ACL) at Argonne National Laboratory. Samples for ICP-OES analysis were prepared by digesting samples in half-concentrated aqua regia or in half-concentrated $\text{H}_2\text{SO}_4\text{:H}_2\text{O}_2$ (3:1).

Electrospray ionization mass spectrometry was performed using Agilent 1100 LC/MSD mass-spectrometer. Samples were prepared by dissolving Na_3AsS_3 and $(\text{NH}_4)_3\text{AsS}_3$ in water at a concentration of ~ 2 mg/mL.

VI. Electrophoretic mobility and surface charge density.

The electrophoretic mobility μ of a charged colloidal sphere is related to its ζ -potential through Henry's equation.^{21,22}

$$\mu = \frac{2\varepsilon_0\varepsilon\zeta f(\kappa r)}{3\eta}, \quad (1)$$

where $f(\kappa r)$ is a dimensionless, monotonically varying function, r is a hydrodynamic radius of a sphere, ε_0 is vacuum permittivity, ε is the dielectric constant and η is the solvent viscosity, κ is Debye-Hückel parameter, which determines the thickness of the diffuse double layer (κ^{-1} , Debye screening length). $f(\kappa r)$ increases from 1.0 at $\kappa r \ll 1$ (Hückel limit) to 1.5 at $\kappa r \gg 1$ (Smoluchowski limit).

A simple equation for estimating $f(\kappa r)$ in the whole range of κr was derived by Ohshima:²³

$$f(\kappa r) = 1 + \frac{1}{2(1 + 2.5/[kr\{1 + 2\exp(-\kappa r)\}])^3} \quad (2)$$

The Debye screening length is determined as:

$$\kappa^{-1} = \left(\frac{\varepsilon_0 \varepsilon k_B T}{e^2 2N_A I} \right)^{1/2}, \quad (3)$$

where N_A is Avogadro number and I is solution ionic strength. $I = \frac{1}{2} \sum c_i z_i^2$, c_i and z_i are the concentration (in mol/m³) and valency of i -th ions, determining the solution ionic strength. For a simplest case, when all ions in solution originate from dissociation of counterions from surface bound ligands (e.g. monovalent Na⁺ from surface-bound Na₃AsS₃), the solution ionic strength is determined as $0.5 \cdot c_{NC} \cdot Z$, where c_{NC} and Z are the concentration and charge of NCs.

The surface charge density is thus determined from experimentally determined ζ -potential and κ :

$$\sigma = \varepsilon_0 \varepsilon \zeta (1 + \kappa r) / r \quad (4)$$

Note that the surface charge density obtained from (4) correspond to the “plane of shear”, which is ~ 0.5 nm or so from the Stern layer, which is an actual nanocrystal surface. The charge at the Stern layer in this case is somewhat higher, though can't be measured directly.

From the Eqs. (1) and (4), the mobility is related to the Debye screening length and surface charge density as:

$$\mu = \frac{2\sigma f(kr)}{3\eta(1+kr)} \quad (5)$$

The corresponding average surface charge of each sphere, Z (in units of e) can be calculated from:

$$\sigma = \frac{Ze}{4\pi r^2} \quad (6)$$

The hydrodynamic radii r were estimated from the dynamic light scattering or by adding the ligand shell thickness (0.6 nm for AsS_3^{3-} , 1.8 nm for $\text{DDA}^+-\text{AsS}_3^{3-}$) to the size estimated from TEM images. For ~ 10 nm PbS NCs these numbers agree well.

(i) **PbS- AsS_3^{3-} -NCs in FA in the presence of excess Na_3AsS_3 .** The solution contains 0.04 mol/L Na_3AsS_3 , which is >10 times higher than required to coordinate all Pb surface sites in PbS NCs ($r=5.6$ nm). Using $\varepsilon=109$ for FA, the Debye screening length, κ^{-1} , is 2.297 nm and $kr=2.438$. Thus, $f(kr)$ from Eq.2 is 1.0761. With the measured mobility of $1.8 \cdot 10^{-8} \text{ m}^2 \text{ V}^{-1} \text{ s}^{-1}$ and $\eta(\text{FA})=3.3 \cdot 10^{-3} \text{ kg m}^{-1} \text{ s}^{-1}$, $\zeta \approx 86$ mV (Eq. 1) the surface charge density is 0.0508 C/m^2 (Eq. 5), corresponding to $Z \approx 125e$ (Eq. 6).

(ii) **PbS- AsS_3^{3-} -NCs in FA purified from excessive Na_3AsS_3 concentration.** For this solution, $I \sim 1$ mol/m³, $\kappa^{-1} \sim 13.6$ nm, $\sigma \approx 0.0133 \text{ C/m}^2$, $\zeta \approx 55$ mV and $Z \approx 33e$.

(iii) **PbS- AsS_3^{3-} -DDAB NCs in toluene.** In this case the electrolyte concentration is negligibly small, leading to the large screening length. Thus, for $\kappa r \ll 1$ (Hückel limit), $f(kr) \sim 1$. From Eq. (1), (4) and (6) we obtain:

$$\mu = \frac{2\varepsilon_0\varepsilon\zeta f}{3\eta} = \frac{2\sigma r}{3\eta} = \frac{Ze}{6\pi\eta r} \quad (7)$$

From the measured electrophoretic mobility of $0.0218 \cdot 10^{-8} \text{ m}^2 \text{ V}^{-1} \text{ s}^{-1}$ (Figure 1B), $\eta_{\text{toluene}}=0.5542 \cdot 10^{-3} \text{ kg m}^{-1} \text{ s}^{-1}$ and $r=6.8$ nm, Z is $\sim 0.05e$.

VII. Fabrication and characterization of nanocrystal-based field effect transistors.

Samples for electrical measurements were prepared by depositing thin films of NCs by drop-casting on highly doped Si wafers with a 110 nm thick SiO_2 thermal gate oxide. Source and drain Ti/Au (70/450Å) electrodes were patterned on the SiO_2 surface by photolithography. Samples were annealed at 300-380 °C for 30 min. All electrical measurements were performed using Agilent B1500 semiconductor parameter analyzer. All room temperature electrical measurements were performed under dry nitrogen atmosphere. At low V_D , I_D increases linearly with V_D (linear regime):²⁴

$$I_D = \frac{WC_i\mu_{lin}}{L} \left(V_G - V_T - \frac{V_D}{2} \right) V_D$$

where L is the channel length, W is the channel width, C_i is the capacitance per unit area of the insulating layer, V_T is the threshold voltage, and μ_{lin} is the linear regime field-effect mobility. μ_{lin} was calculated from the transconductance:

$$g_m = \left. \frac{\partial I_D}{\partial V_G} \right|_{V_D=const} = \frac{WC_i V_D}{L} \mu_{lin}$$

by plotting I_D vs. V_G at a constant low V_D , with $V_D \ll (V_G - V_T)$ (Figure S11A). The slope of this plot is equal to g_m .

For $V_D > (V_G - V_T)$, I_D tends to saturate due to pinch-off of the accumulation layer (saturation regime). This case is approximately described by the equation

$$I_D = \frac{WC_i\mu_{sat}}{2L} (V_G - V_T)^2$$

μ_{sat} was calculated from the slope of $\sqrt{|I_D|}$ vs. V_G (Figure S11B).

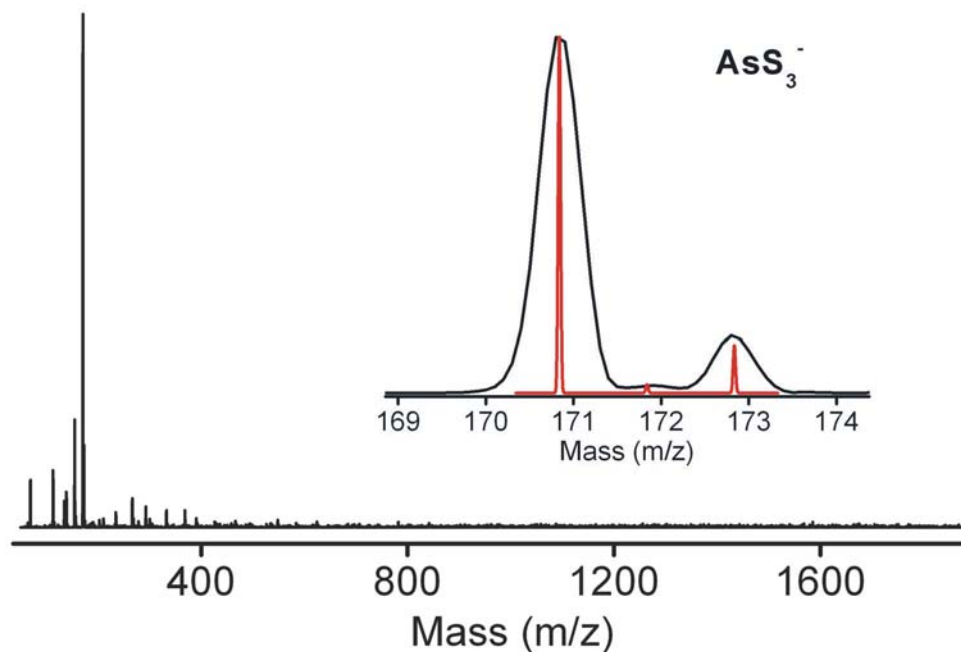


Figure S1. Electrospray ionization mass spectrometry (ESI-MS) of $(\text{NH}_4)_3\text{AsS}_3$ acquired in negative ion-mode using H_2O as a carrier fluid. As expected, no peaks were observed in the positive ion mode. In agreement with the previous reports for anionic Zintl clusters,²⁵ the ions appear with reduced charge of typically -1, due to anion oxidation during the electrospray process. The assignments based on m/z values can be additionally confirmed by comparing experimental mass-spectra with calculated isotope patterns (red line, enlarged spectrum on the right side).

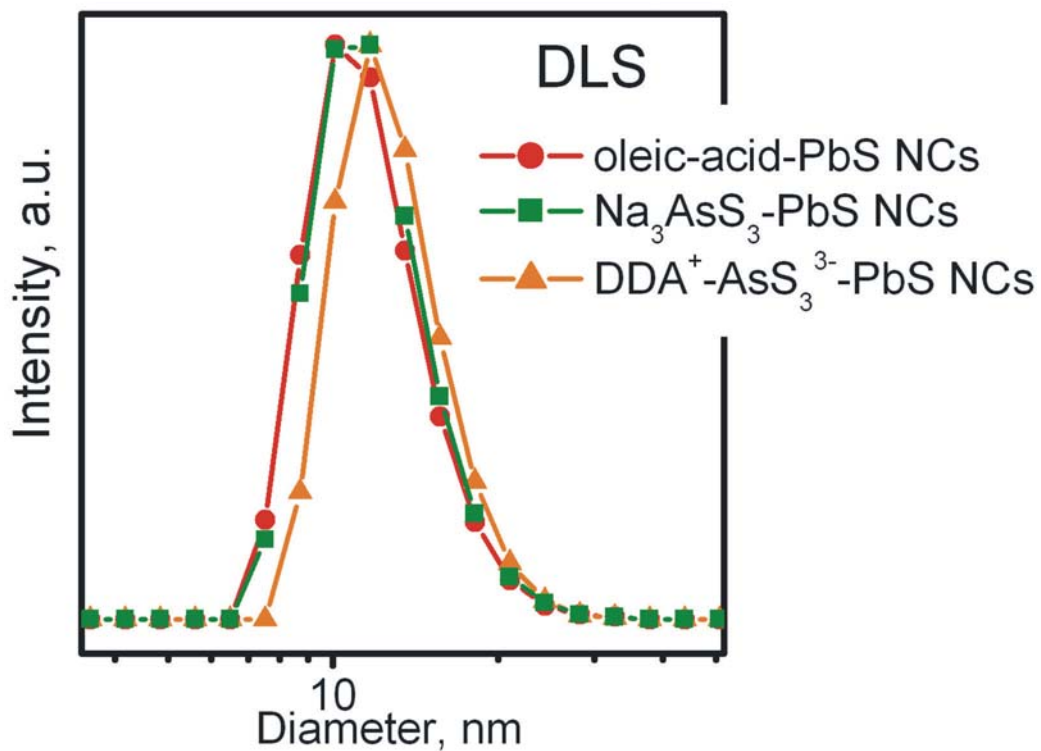


Figure S2. Dynamic light scattering measurements for PbS NCs with ~10 nm core size capped with various ligands: oleic acid in toluene (circles, red), Na_3AsS_3 in FA (squares, green), DDA^+ - AsS_3^{3-} -capping in toluene (triangles, orange).

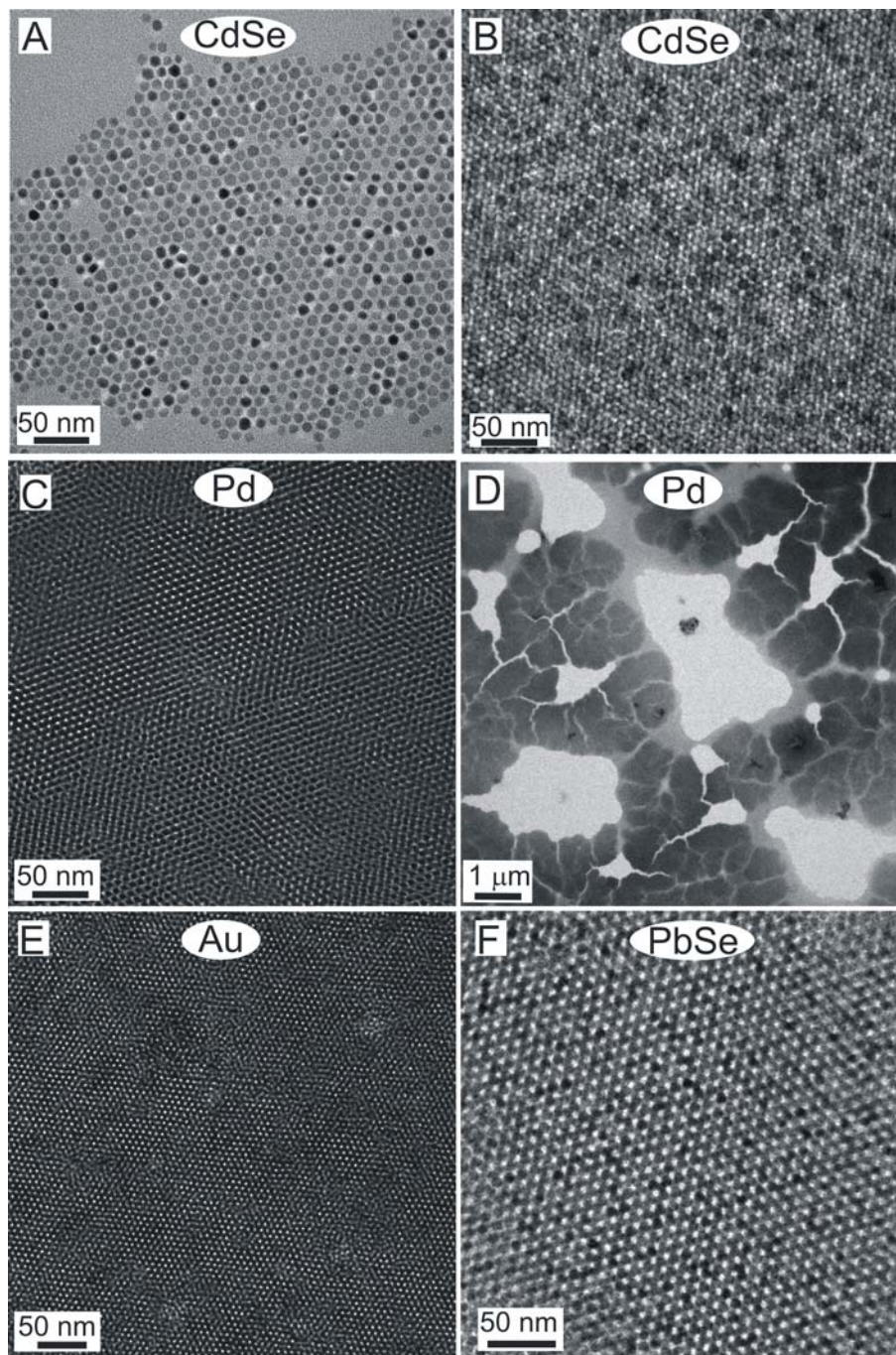


Figure S3. TEM images of 2- and 3-dimensional single-component superlattices composed of DDA^+ - AsS_3^{3-} -capped CdSe NCs (A, ~ 8.1 nm core size, 2-dimensional array), CdSe NCs (~ 10 nm core size, FCC lattice), Pd NCs (C, D, ~ 4.2 nm core size), Au NCs (E, ~ 4 nm core size), and PbSe NCs (F, ~ 8 nm core size).

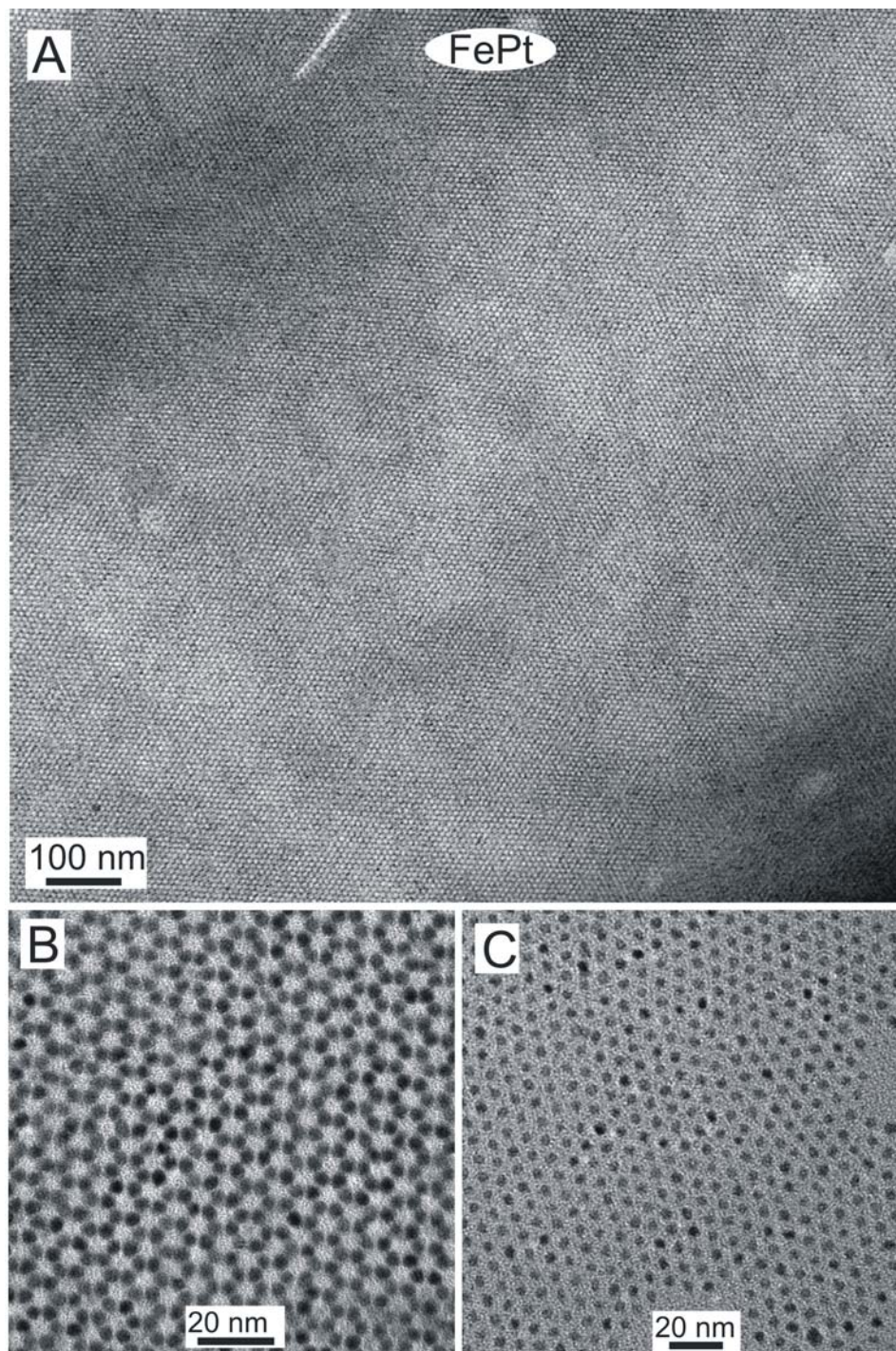


Figure S4. TEM images of single-component superlattices composed of DDA^+ - AsS_3^{3-} -capped FePt NCs. (~ 3.8 nm core size). The low-magnification image (A) represents a large-scale view of hexagonal close packed superlattice shown in (B).

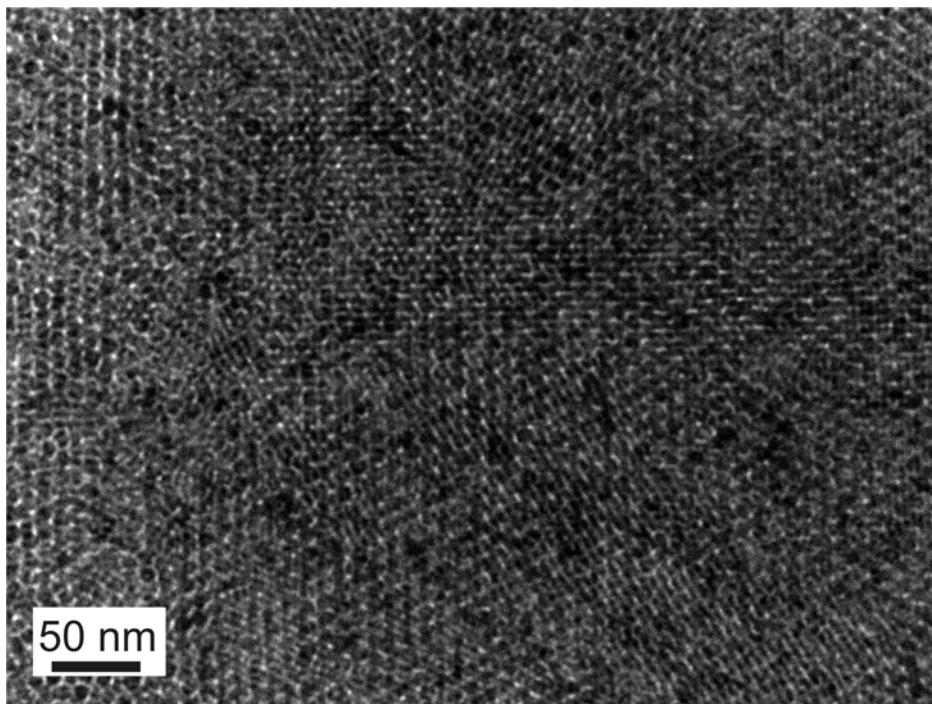


Figure S5. TEM image of single-component superlattices composed of DDA^+ - $\text{Sn}_2\text{S}_6^{4-}$ -capped CdSe NCs. (~10 nm core size).

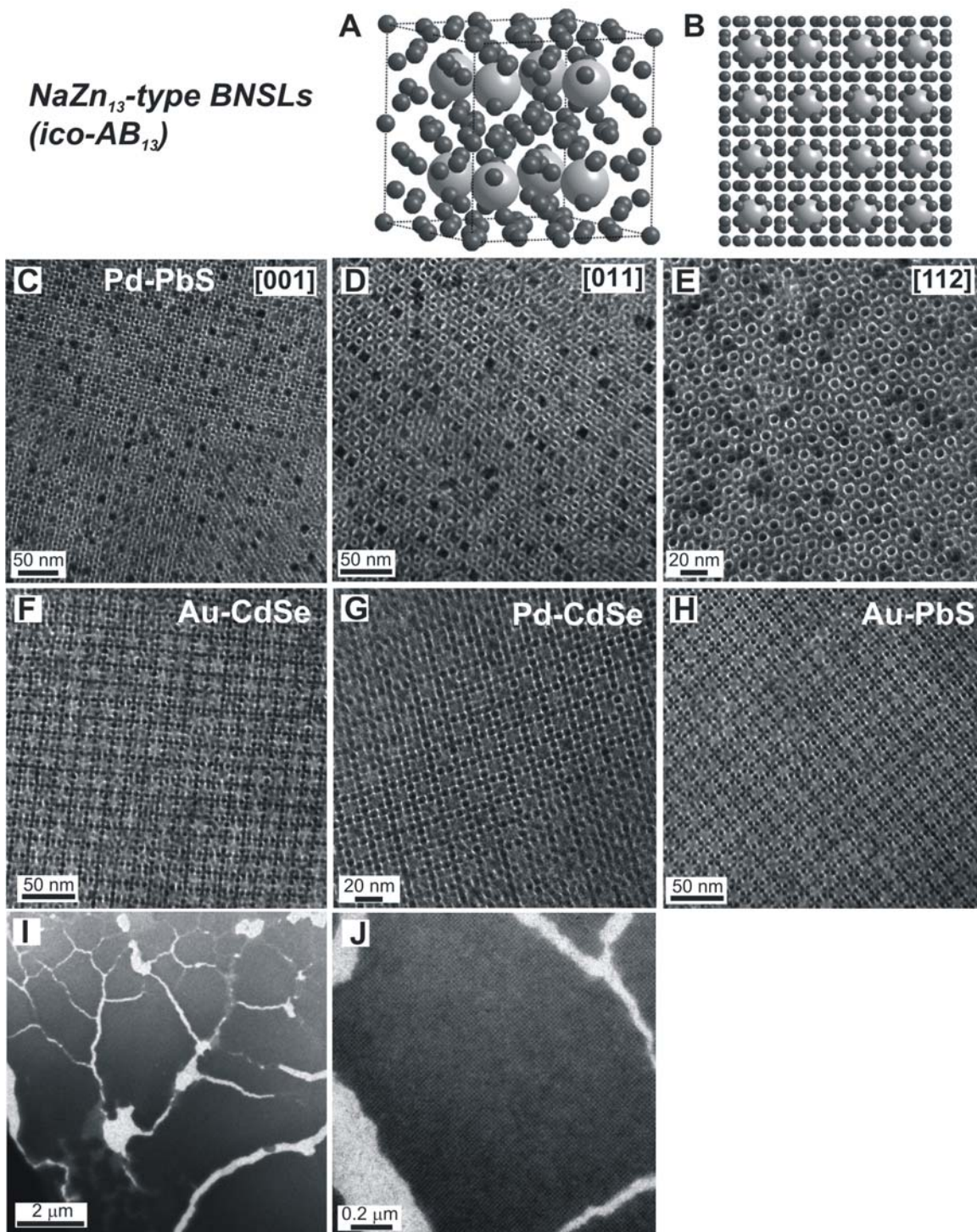
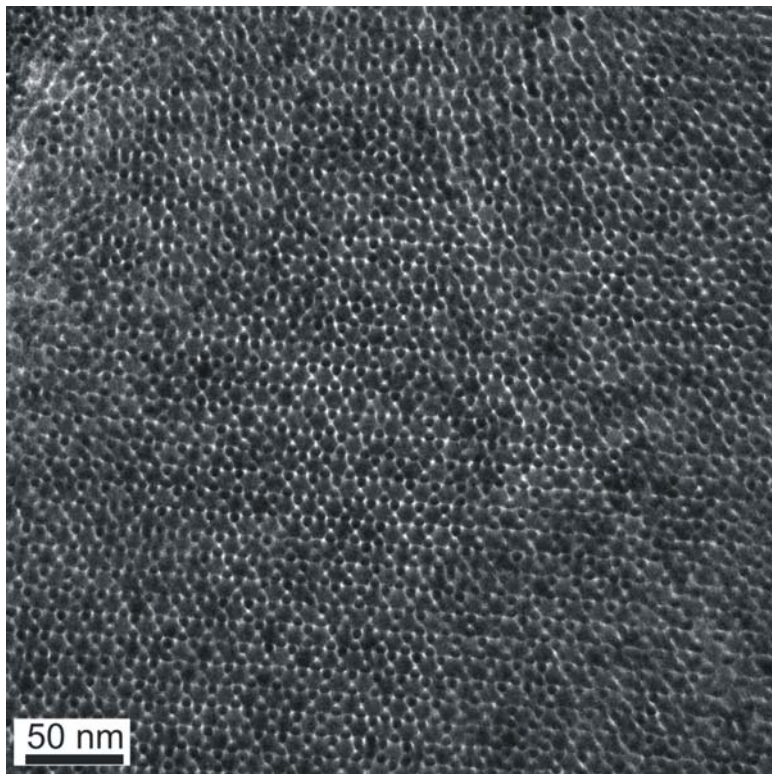


Figure S6. TEM images of binary nanocrystal superlattices with NaZn₁₃-type crystal structure grown from DDA⁺-AsS₃³⁻-capped NCs. (A) Unit cell of NaZn₁₃-type.^{26,27} (B) (001) projection of NaZn₁₃-type lattice. (C, D, E) Different crystallographic projections observed for superlattices composed of 4.2 nm Pd and 10 nm PbS NCs ($\gamma_{\text{eff}} \sim 0.57$); zone axes are shown on each figure. The zone axes assignments are based on the recently report by Murray *et al.*²⁷ (F) Superlattice composed of 4 nm Au and 10 nm CdSe NCs ($\gamma_{\text{eff}} \sim 0.56$). (G) Superlattices composed of 4.2 nm Pd and 10 nm CdSe NCs ($\gamma_{\text{eff}} \sim 0.595$). (H, I, J) Superlattices grown from Au and PbS NCs ($\gamma_{\text{eff}} \sim 0.64$) viewed at various magnifications to illustrate the extend of self-ordered domains.



AlB₂-type

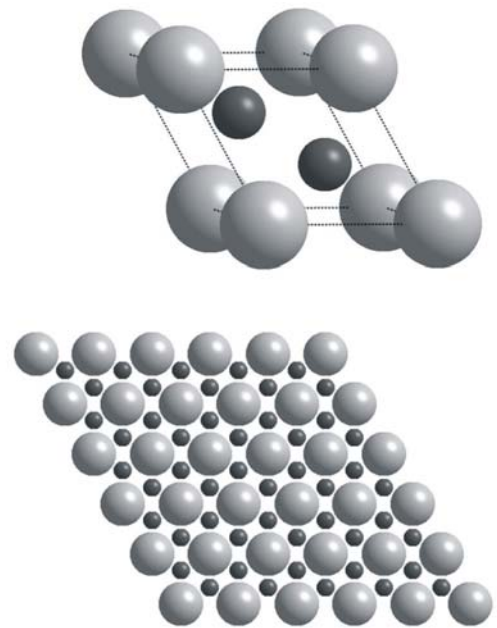


Figure S7. TEM images of a BNSL with AlB₂-type structure grown from DDA⁺-AsS₃³⁻-capped 4 nm Au and 10 nm CdSe NCs ($\gamma_{\text{eff}} \sim 0.56$). Same sample as shown in Figure S6F. On the right: unit cell of AlB₂-type lattice.

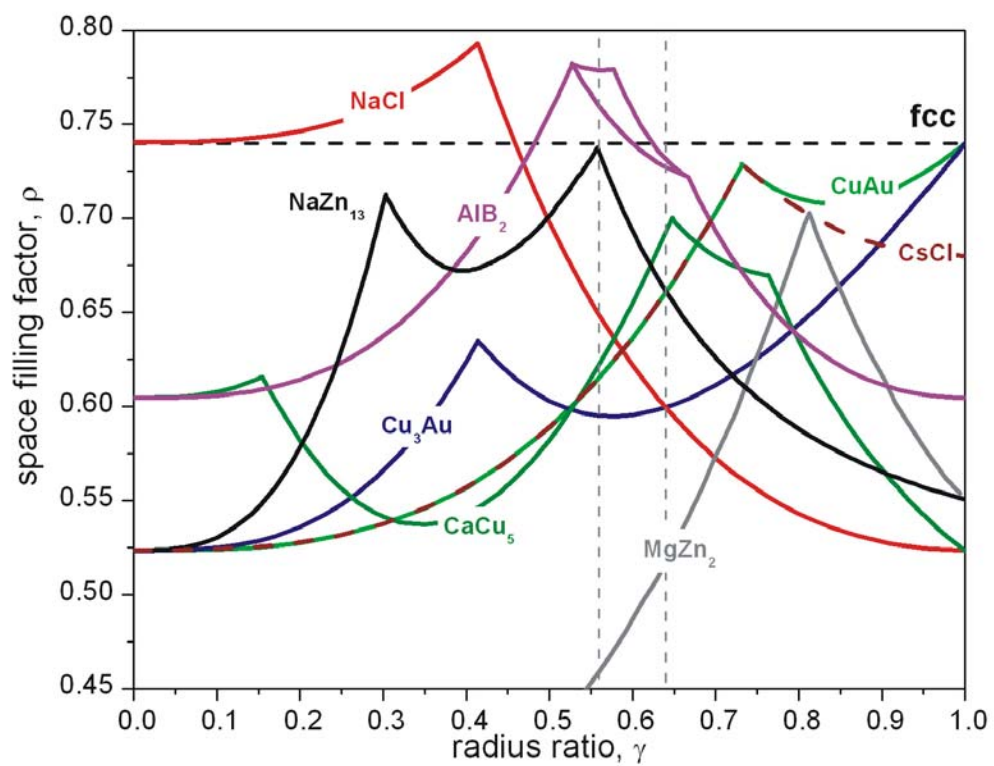


Figure S8. Calculated space-filling curves for NaCl, CsCl, CuAu, AlB₂, MgZn₂, Cu₃Au, CaCu₅ and NaZn₁₃ binary structures. Dashed vertical lines show the values of γ_{eff} studied in this work. The curves were plotted as reported previously.^{16,28}

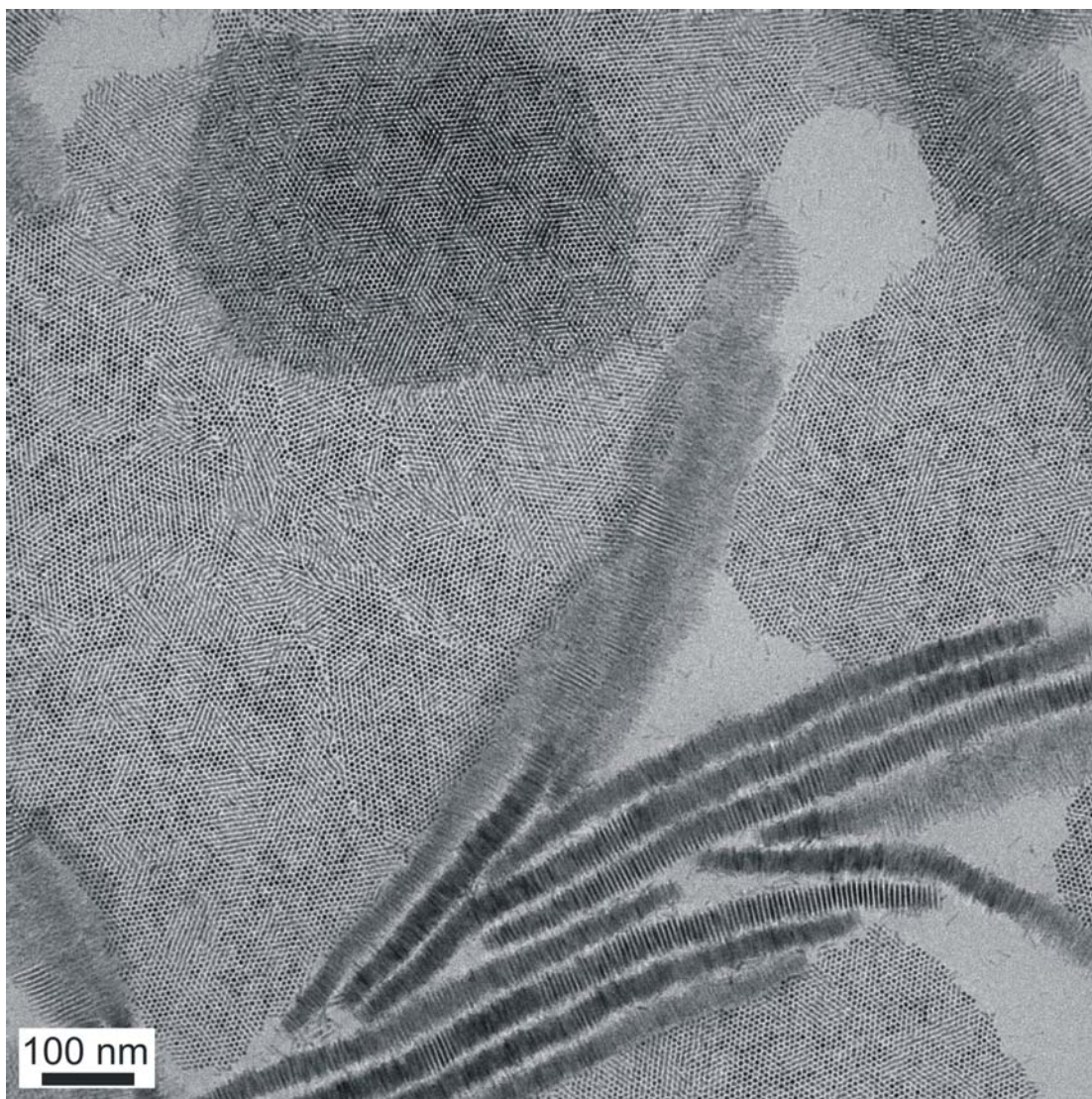


Figure S9. TEM images of self-assembled monolayers and tracks of CdS nanorods capped with conventional organic ligands (octadecylphosphonic acid). The observed structure can be classified as hexatic smectic *B*.

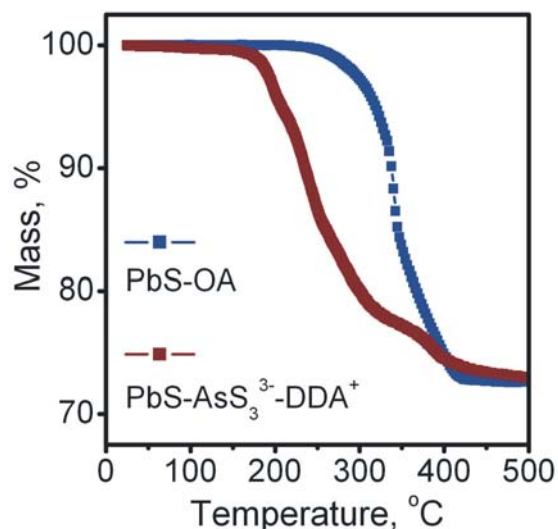


Figure S10. Thermogravimetric analysis measurements for oleic acid-capped PbS NCs (blue) and DDA^+ - AsS_3^{3-} -PbS NCs (red) with $\sim 3.7\text{nm}$ PbS core diameter.

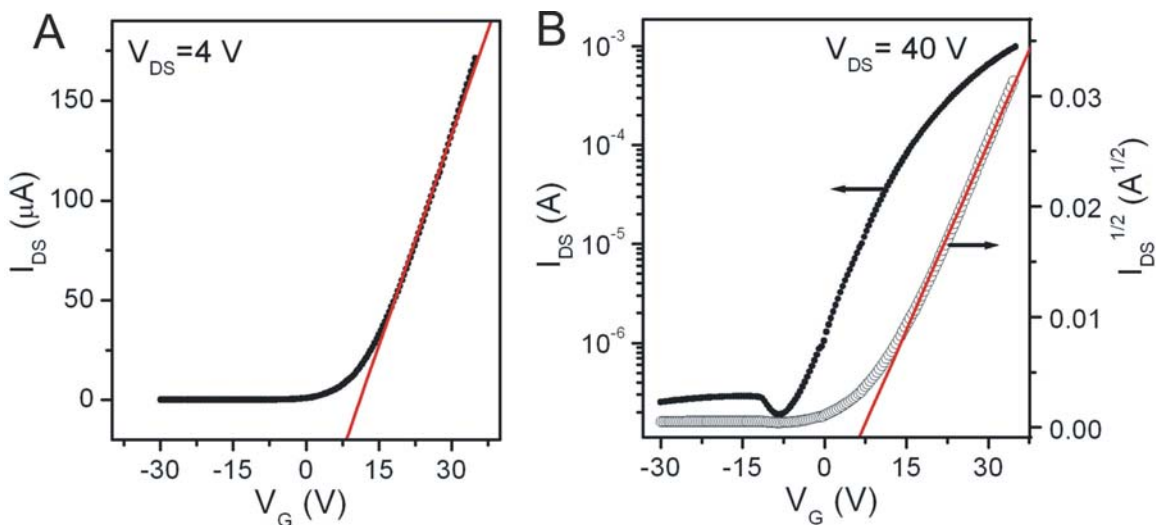


Figure S11. Transfer characteristics (plot of drain current vs. gate voltage) for the FET with the channel fabricated by annealing DDA^+ - $\text{Sn}_2\text{Se}_6^{4-}$ -capped NCs. (A) represents linear regime operation, while (B) shows operation in the saturated mode. Data were collected from the same device as shown in Figure 4B.

References:

- (1) Kim, S. W.; Park, J.; Jang, Y.; Chung, Y.; Hwang, S.; Hyeon, T.; Kim, Y. W. *Nano Lett.* **2003**, *3*, 1289-1291.
- (2) Sun, S.; Murray, C.B.; Weller, D.; Folks, L.; Moser, A. *Science* **2000**, *287*, 1989-1992.
- (3) Peng, S.; Lee, Y. M.; Wang, C.; Yin, H. F.; Dai, S.; Sun, S. H. *Nano Res.* **2008**, *1*, 229-234.
- (4) Talapin, D. V.; Rogach, A. L.; Kornowski, A.; Haase, M.; Weller, H. *Nano Lett.* **2001**, *1*, 207-211.
- (5) Talapin, D. V., Nelson, J.H., Shevchenko, E.V., Aloni, S., Sadtler, B., Alivisatos, A.P. *Nano Lett.* **2007**, *7*, 2951-2959.
- (6) Robinson, R. D., Sadtler, B., Demchenko, D.O., Erdonmez, C.K., Wang, L.-W., Alivisatos, A.P. *Science* **2007**, *317*, 355-358.
- (7) Hines, M. A., Scholes, G. D. *Adv. Mater.* **2003**, *15*, 1844-1849.
- (8) Behrens, H.; Glasser, L. *Z Anorg. Allg. Chem.* **1955**, *278*, 174-183.
- (9) Osman, M. A.; Ernst, M.; Meier, B. H.; Suter, U. W. *J. Phys. Chem. B* **2002**, *106*, 653-662.
- (10) Xie, W.; Gao, Z. M.; Pan, W. P.; Hunter, D.; Singh, A.; Vaia, R. *Chem. Mater.* **2001**, *13*, 2979-2990.
- (11) Heinz, H.; Suter, U. W. *Angew. Chem. Int. Ed.* **2004**, *43*, 2239-2243.
- (12) Heinz, H.; Vaia, R. A.; Farmer, B. L. *Langmuir* **2008**, *24*, 3727-3733.
- (13) Beck, J. S.; Vartuli, J. C.; Roth, W. J.; Leonowicz, M. E.; Kresge, C. T.; Schmitt, K. D.; Chu, C. T. W.; Olson, D. H.; Sheppard, E. W.; McCullen, S. B.; Higgins, J. B.; Schlenker, J. L. *J. Am. Chem. Soc.* **1992**, *114*, 10834-10843.
- (14) Kresge, C. T.; Leonowicz, M. E.; Roth, W. J.; Vartuli, J. C.; Beck, J. S. *Nature* **1992**, *359*, 710-712.
- (15) Shevchenko, E. V., Talapin, D. V., Murray, C. B., O'Brien, S. *J. Am. Chem. Soc.* **2006**, *128*, 3620-3637.
- (16) Bodnarchuk, M. I.; Kovalenko, M. V.; Heiss, W.; Talapin, D. V. *J. Am. Chem. Soc.* **2010**, in print.
- (17) Yu, W. W.; Qu, L. H.; Guo, W. Z.; Peng, X. G. *Chem. Mater.* **2003**, *15*, 2854-2860.
- (18) Cademartiri, L.; Montanari, E.; Calestani, G.; Migliori, A.; Guagliardi, A.; Ozin, G. A. *J. Am. Chem. Soc.* **2006**, *128*, 10337-10346.
- (19) Moreels, I.; Lambert, K.; De Muynck, D.; Vanhaecke, F.; Poelman, D.; Martins, J. C.; Allan, G.; Hens, Z. *Chem. Mater.* **2007**, *19*, 6101-6106.
- (20) Moreels, I.; Lambert, K.; Smeets, D.; De Muynck, D.; Nollet, T.; Martins, J. C.; Vanhaecke, F.; Vantomme, A.; Delerue, C.; Allan, G.; Hens, Z. *ACS Nano* **2009**, *3*, 3023-3030.
- (21) Henry, D. C. *Proc. R. Soc. Lond. A* **1931**, *133*, 106-129.
- (22) Hunter, R. J. *Foundations of Colloid Science*; 2nd ed.; Oxford University Press: New York, 2001.
- (23) Ohshima, H. *J. Colloid Interface Sci.* **1996**, *179*, 431-438.
- (24) Kagan, C. R.; Andry, P. *Thin Film Transistors*; Marcel Dekker: New York, 2003.
- (25) Goicoechea, J. M.; Sevov, S. C. *Organometallics* **2006**, *25*, 4530-4536.
- (26) Shevchenko, E. V.; Talapin, D. V.; O'Brien, S.; Murray, C. B. *J. Am. Chem. Soc.* **2005**, *127*, 8741-8747.
- (27) Chen, J.; Ye, X. C.; Murray, C. B. *ACS Nano* **2010**, *4*, 2374-2381.
- (28) Murray, M. J.; Sanders, J. V. *Philos. Mag. A* **1980**, *42*, 721-740.